Study of a Position Sensing Gas Proportional Detector for Decommissioning

A Thesis Presented for the

Master of Science

Degree

The University of Tennessee, Knoxville

Christopher Echterling

May 2020

Acknowledgements

Many people have helped me in my pursuit of this project and deserve my gratitude. First, I would like to thank my advisor, Dr. Jason Hayward, for taking on a distance student with a busy career and an idea for a difficult project. Thank you to Dr. Lawrence Heilbronn and Dr. Eric Lukosi for serving on my committee. I would also like to thank the faculty that taught distance courses that enabled me to pursue this degree and were understanding when my travel schedule made things difficult, and the Nuclear Engineering staff that found ways to enable me to access the resources I needed on nights and weekends to accomplish my work. I truly appreciate the patience everyone has had as I very slowly worked my way through this degree and project.

Thank you to Dr. Richard Riedel at Oak Ridge National Laboratory for answering my questions about preamplifiers for position sensing gas proportional detectors. Thank you also to Dr. Bruno Guerard at Institut Laue-Langevin for working through my detector design with me.

I also need to thank my colleagues at Chase Environmental Group for all the ideas and advice on this project.

Finally, I need to thank my fiancée Jamie Herold for supporting my pursuit of this degree and project and tolerating all the late nights and weekends spent on homework and research.

Abstract

Decontamination and decommissioning as required by the Nuclear Regulatory Commission is guided by the Multi-Agency Site Survey and Investigation Manual. This manual lays out the types of radiological surveys required for decommissioning and the methods and equations to analyze the data. By optimizing detectors based on this manual, a business engaged in providing decommissioning services can become more competitive.

To optimize a detector for decommissioning, position-sensing gas proportional detectors were investigated to determine critical design criteria. Gas proportional detectors are already commonly in use for decommissioning work. By adding position sensing, additional speed and efficiency of surveying can be gained.

Position-sensitive gas proportional designs appropriate for the application of interest were reviewed. Some of the critical design parameters for the anode include the diameter, the resistance, the capacitance, and the tension that can be applied to the anode. The counting gas and pressure and applied bias voltage are required to calculate the gas amplification.

A prototype detector was constructed using a resistive anode with the intent to use charge division to sense position and these design criteria were investigated more fully. A one meter long by 10 centimeter wide detector with five resistive anodes in a planar configuration was constructed. Anode capacitance must be carefully controlled to ensure

that the anode tension is sufficiently high to prevent detector sparking at voltages large enough to ensure gas amplification is on the order of 10^2. The intrinsic noise of the detector is problematic and requires careful preamplifier design and specification. The preamplifiers should be designed in conjunction with the detector to ensure optimal functionality.

Table of Contents

List of Tables

List of Figures

Chapter 1

Introduction and General Information

Decommissioning of Licensed Facilities

Decontamination and decommissioning (D&D) is required by the Nuclear Regulatory Commission (NRC) as described in 10 CFR 20 Subpart E (Radiological Criteria for License Termination). The NRC uses risk-based criteria for license termination, specifying the Total Effective Dose Equivalent (TEDE) limits in order to release a site from license controls. As stated in 10 CFR 20.1402 Radiological Criteria for Unrestricted Use:

"A site will be considered acceptable for unrestricted use if the residual radioactivity that is distinguishable from background radiation results in a TEDE to an average member of the critical group that does not exceed 25 mrem (0.25 mSv) per year, including that from groundwater sources of drinking water, and the residual radioactivity has been reduced to levels that are as low as reasonably achievable (ALARA). Determination of the levels which are ALARA must take into account consideration of any detriments, such as deaths from transportation accidents, expected to potentially result from decontamination and waste disposal."

Because the criteria used are risk based, licensees must consider all exposure pathways and model the expected doses to the critical group based on the residual surface and volume radioactivity at their site. Volumetric contamination, such as neutron or proton activation of structural materials at particle accelerator or nuclear reactor facilities, can be measured and modeled in a variety of ways depending on the matrix and future use scenario. Methods used may include direct measurement of gamma emissions or sampling and laboratory analysis.

Surface contamination is usually measured directly in the field using portable instruments. Charged particle emissions are preferred targets of measurement in most cases. Situations where surface contamination exists without proton or neutron activation of the underlying substrate occur frequently in academic and industrial research facilities engaged in biological, chemical and/or medical work. The isotopes usually encountered in those situations consist of what is colloquially known as "CHIPS": Carbon-14, Hydrogen-3, Iodine-125, Phosphorus-32, Phosphorus-33, and Sulfur-35. Another common situation where surface contamination exists without activation is former radium research facilities. Common isotopes in these situations include the Uranium series and the Thorium series in whole or in part.

Survey Design

Survey design for the decommissioning of licensed facilities is most frequently guided by the Multi-Agency Radiation Survey and Site Investigation Manual (MARSSIM) (United States Department of Defense, Department of Energy, Environmental Protection Agency, and Nuclear Regulatory Commission, 2000). In general, surveys begin with a scan survey to identify any elevated areas of contamination. Elevated areas are assessed with a static timed count as well as a removable contamination measurement. Finally, a systematic survey of static timed counts and removable contamination measurements is performed in random locations throughout the survey unit. The random locations may be random x and random y for areas least likely to be contaminated, or they may be a grid pattern with fixed distances between survey points, based on a random starting point within the survey unit.

Surveys must be designed to detect contamination levels below the limits determined by dose modeling. For a MARSSIM survey design, these limits are referred to as the Derived Concentration Guideline Limits (DCGL). The NRC publishes a set of limits based on very conservative assumptions in the pathway analysis and dose modeling. These limits are known as Default Screening Values (DSV). Scan surveys should be designed to have a Minimum Detectable Concentration (MDC) well below the DCGL whenever possible to ensure that contamination is found during remediation, rather than at the Final Status Survey (FSS). Finding areas of missed contamination during the FSS can result in costly schedule delays during a decommissioning project. As a result, optimizing scan surveys can result in efficiencies and competitive advantage.

Minimum Detectable Concentration for Scan Surveys

The MDC equation for beta/gamma scan surveys can be found in MARSSIM Chapter 6. The minimum detectable number of source counts during time interval i is s_i, found using Equation 1. The time interval, i, is the amount of time it takes to pass the detector over the contamination. The number of background counts during that time is denoted b_i. The level of performance for false positives versus true positives is d'.

$$s_i = d'\sqrt{b_i} \quad (1)$$

The value of s_i is used to find the Minimum Detectable Count Rate using Equation 2.

$$MDCR = s_i * (60/i) \quad (2)$$

The Scan MDC in Equation 3, in dpm / 100 cm^2, is found by dividing the resulting MDCR by the square root of the surveyor efficiency, p, the instrument efficiency, ε_i, the surface efficiency, ε_s, and the area of the detector, A, divided by 100 cm^2.

$$ScanMDC = \frac{MDCR}{\sqrt{p} * \varepsilon_i * \varepsilon_s * \frac{A}{100\ cm^2}} \quad (3)$$

From these equations, it is evident that reducing the background count rate, increasing the instrument efficiency, increasing detector area, and/or increasing surveyor efficiency will all result in faster scan rates or lower minimum detectable concentrations, resulting in a more competitive survey design.

Decreasing the background count rate and increasing detector efficiency is not easily accomplished. Avoiding the use of intrinsically radioactive materials like lead based solder can help reduce background, as can the use of low atomic number (Z) materials for detectors designed for counting charged particles instead of photons.

There is a practical limit to how much the detector area can be increased. With a large area detector, if a small spot of contamination is scanned, a second technician with a smaller detector will be necessary to more accurately and precisely locate and measure the spot of contamination. A detector design that can not only detect and measure the activity of the spot of contamination, but also sense where the interaction occurred within the detector would alleviate the need for resurveying with a small detector.

Gas proportional detectors tend to be the preferred choice for decommissioning for a number of reasons. Proportional detectors are efficient at detecting charged particles, they can discriminate between alphas and betas, and they can be made in a variety of sizes. Therefore, the goal of this thesis is to investigate a potential design of a position sensing gas proportional detector for beta particle detection and measurement for the purpose of decommissioning surveys.

This thesis will review the basic concepts of gas filled radiation detectors, and in particular, position sensing gas proportional detectors in Chapter 2. The design considerations of the first phase of constructing a prototype gas proportional detector will be discussed in Chapter 3. Test results for the first prototype detector, including unforeseen challenges will be presented in Chapter 4. Chapter 5 will outline key points for the next iteration of a prototype detector.

Chapter 2

Literature Review

Gas Filled Detectors

A variety of detectors exist based on the principle of ionizing molecules of gas between two electrodes. This can be an open volume or a closed chamber. A bias voltage is applied to create an electric field. If the field is such that the ions created by the incident radiation travel towards the respective electrodes prior to recombination, the current can be measured. This type of detector is known as an ion chamber (Rossi & Staub, 1949).

If the bias voltage is increased further, such that the electrons created by the incident radiation travel towards the electrodes with enough energy to create additional ionization events in proportion to the original energy of the incident radiation, an amplified signal is created. This type of detector is known as a proportional counter. If the voltage is increased further such that the ions create so many additional ionizations that the signal pulse is identical regardless of the energy or type of incident radiation, this type of detector is known as a Geiger Mueller (GM) detector (Rice-Evans, 1974). While ion chambers are typically operated in current mode, proportional counters and GM detectors are typically operated in pulse mode (Knoll, 2010).

The signal generated in all three of these detectors depends on the flow of ions, and not upon the collection of electrons at the anode or positive ions at the cathode. The movement of ions induces current (Ramo, 1939) (Shockley, 1938).

Proportional Counters

Proportional counters are frequently used for alpha, beta, x-ray and neutron detection and energy measurements depending on design and fill gas (Knoll, 2010). The typical configuration of a proportional counter is a cylinder cathode and a very thin wire anode (Rice-Evans, 1974). However, other configurations are possible. Charpak created proportional counters using multiple anode wires in the same volume and treated each anode wire as a separate detector. By measuring which wires produced a pulse and where the largest pulses occurred, the position or track of the ionizations could be measured (Charpak, Rahm, & Steiner, 1970).

Fill Gas

A variety of gasses can be used to fill a proportional counter. Commonly, noble gasses such as argon are used. As the positive ions of a pure noble gas are collected at the cathode, electrons from the cathode will neutralize the positive ions. The energy released in this process may be enough to cause an electron emission, causing a new avalanche to begin. Another possibility is the emission of ultraviolet photons during an avalanche. By mixing a small amount of polyatomic gas with the noble gas, these effects can be quenched (Rice-Evans, 1974). A common mixture is 90% argon and 10% methane, also known as P10 (Knoll, 2010). P10 gas requires approximately 26 eV to create an ion pair. The energy required to ionize a fill gas is typically denoted by W (Wolff, 1974).

Gas Amplification

In a proportional counter, the electric field is large enough that the electrons created by the initial radiation are sufficiently energetic to create additional ions. These additional electrons create further ions, in an avalanche that proceeds exponentially. This is called the Townsend Avalanche (Knoll, 2010). The additional gain due to the Townsend Avalanche is called gas multiplication (Rossi & Staub, 1949). Ward Diethorn (Diethorn, 1956) was able to derive an equation and parameters for gas multiplication in his proportional counter. Richard Wolff (Wolff, 1974) measured the parameters for additional fill gas mixtures.

Energy Resolution

When calculating the energy resolution using Poisson statistics, the expected variance in the number of ions created in a material by a given energy of radiation is larger than the experimentally observed variance in the number of ions created. This is accounted for by use of the Fano factor (Fano, 1947). Fano factors differ for various fill gasses and mixtures, ranging from $F = 0.26$ for pure methane, $F = 0.17$ to 0.19 for argon, and $F = 0.17$ to 0.19 for an argon and methane mixture (Alkhazov, Komar, & Vorob'ev, 1967).

Another impact on energy resolution is the space charge effect. As the gas is ionized, the electrons move rapidly to the anode leaving a large cloud of positive ions that can distort the electric field in varying ways. The general space charge effect can become more serious as counting rates increase and areas of positive ions grow larger (Hendricks, 1969). The self-induced space charge effect occurs during a single avalanche and can reduce the rate of ion production normally expected during that avalanche (Mori, Uno, & Watanabe, 1982).

In general, to reduce the impact of the space charge effect, the detector should be operated at a low gas amplification, on the order of 10^2 (Hendricks, 1969). The self-induced space charge effect depends on anode wire diameter, gas pressure, and incoming radiation energy (Mori, Uno, & Watanabe, 1982).

Position Sensing

A few methods of position sensing exist for proportional counters. The first method, previously mentioned, is using the multiwire proportional counter. By creating a detector with multiple anode wires, the position of an interaction can be determined by examining which anode wire produced a pulse. If the interaction is registered on one wire, that wire will produce a negative pulse as the positive ions flow away from the anode and the adjacent wires will produce positive pulses as the positive ions flow towards them and towards the cathodes (Charpak, Rahm, & Steiner, 1970). The signal pulses, whether positive or negative, are induced by the movement of the ions in the detector and not by actually collecting the electrons (Shockley, 1938) (Ramo, 1939). The negative pulse indicates which wire detected the event and this determines the position along one axis. To determine position along two axes in a multiwire proportional counter, orthogonal planes of anode wires are used. If the cathode planes are constructed of wires instead of solid plates, attempts have been made to detect the positive pulses on those wires and use that to resolve the position along the second axis (Charpak, Rahm, & Steiner, 1970).

A second method of sensing position with a proportional counter is using a resistive anode wire. Resistive anode wires can be used in both single wire detectors as well as multiwire proportional counters. The first coordinate in a multiwire proportional counter is measured in the usual way, and the second coordinate is measured along the resistive anode (Foeth, Hammarstrom, & Rubbia, 1973) (Schubelin, et al., 1975).

The primary methods used to measure position with resistive anode wires are charge division (Alberi & Radeka, 1976) and the rise time method (Borkowski & Kopp, 1968). The charge division method offers some advantages in that it does not depend on charge collection time, electrode resistance uniformity, or electrode capacitance uniformity (Alberi & Radeka, 1976). The charge division method requires a charge integrating preamplifier at each end of each anode using capacitive decoupling for the best noise performance (Alberi & Radeka, 1976).

In charge division, the total amount of charge produced in the detector, as sensed by the anode wire, is the sum of the signal output from each end of the anode, as measured by the charge integrating preamplifiers. The position of interaction along the anode wire is then determined by dividing the signal output from one end of the anode by the summed signal output of both ends of the anode multiplied by the length of the anode (Alberi & Radeka, 1976).

Chapter 3

Materials and Methods

Detector Design Details

Nuclides of Concern

The primary function of this design is to detect beta particles. Alpha particle detection is also useful, but outside the scope of the current design iteration. Alpha contamination scanning relies on a different set of assumptions and uses a different set of MDC equations for scanning (United States Department of Defense, Department of Energy, Environmental Protection Agency, and Nuclear Regulatory Commission, 2000).

Generally, C-14 will be the lowest energy beta emitter commonly encountered. It is prevalent in a variety of life science research in university, pharmaceutical, and other chemical industries. The highest energy beta emitter commonly encountered is Y-90 (found in equilibrium with Sr-90). Common beta emitters, their end point beta emission energies, and their highest probability beta emissions are shown in the table below (Table 1). If the detector is responsive to betas as low as 49 keV and as high as 2279 keV, it will be effective for most of the isotopes commonly encountered in decommissioning. The exception is H-3. However, due to the very low energy of H-3, it is difficult to detect with portable instrumentation, unless the detector is of a windowless design. Windowless detectors have proven to be very difficult to use in field conditions. As a result, H-3 is typically measured only by removable contamination measurements with liquid

Table 1: Beta Emitting Isotopes and Energies

Nuclide	Beta Average Energy (keV)	Beta Maximum Energy (keV)
Hydrogen-3 (Be, 2006)	5.68	18.564
Carbon-14 (Be M.-M. a., 2013)	49.16	156.476
Cobalt-60 (Be M.-M. a., 2006)	95.6	317.32
Technetium-99 (Be, et al., 2004)	94.6	293.8
Yttrium-90 (Be M.-M. a., 2006)	926.7	2278.7

scintillation counting and is excluded as a nuclide for consideration in this detector design.

Detector Shape and Material

A planar detector was designed to allow for efficient scanning surveys of large areas of contaminated surfaces (e.g. unobstructed floors and walls). As surface contamination is customarily measured in units of disintegrations per minute (dpm) per 100 cm^2, the detector was designed to have a detection area of 100 cm by 10 cm.

Initially, Ultra High Molecular Weight Polyethylene (UHMW) was chosen to construct the detector body as extrusions are readily available in the appropriate size. UHMW has been used to make impact and abrasion resistant protective devices for other detectors with great success. Additionally, for an alpha and beta particle detector, the very low effective Z-number of the material helps ensure a lower gamma background. However, difficulties in machining more complex shapes and the instability due to internal stresses of commonly available extrusions ultimately made this an unrealistic material choice.

Aluminum and stainless steel are more widely used materials for detectors. Aluminum alloys have a much lower Z-number than stainless steels, reducing the gamma background in comparison. Aluminum alloys also have a much lower density than stainless steels and given that much of the detector body size considerations are not structural, but instead chosen for other manufacturing and assembly considerations, aluminum results in a lighter weight instrument for field use.

The body of the detector will also serve as the cathode. For this reason, a material with good conductivity is important. The common aluminum alloys have comparable conductivity, as seen in the following table (Table 2) (ASM International, 1990). For the body of the detector, 6061-T6 offers the lowest density, highest electrical conductivity, and a sufficient tensile strength.

The back plane of the detector serves as one of the cathodes, the mounting points for the anode buss bars, and feedthroughs for gas and signal connectors. Hermetically sealed BNC bulkhead connectors from Pasternack Enterprises were chosen. These connectors have a maximum panel thickness of 0.311" (Pasternack Enterprises, Inc, 2017). This serves as the maximum material condition (MMC) for the backplane thickness. To maintain compatibility with existing instrumentation systems, 1/8" NPT gas fittings were chosen. For 1/8" NPT threads, the minimum length of engagement of the threads is 0.1615" but, joints should be further tightened to ensure a leak free connection (American Society of Mechanical Engineers, 2013). Nylon 6/6 hex standoffs were selected to insulate the anode buss bar from the backplane. These standoffs use M3x0.5 threads and have thread length of 4.7 mm (0.1850"). The threaded holes for the standoffs must be blind holes to ensure that there is no gas leakage. If the hole is drilled with a 118° twist drill of 2.5 mm diameter, then the total hole depth will be 4.7 mm + 0.75 mm = 5.45 mm (0.215"). The Least Material Condition (LMC) must therefore be greater than 0.215". A nominal backplane thickness of 1/4" was chosen.

Table 2: Properties of Common Aluminum Alloys

Alloy	Density (g/cm3 at 20C)	Electrical Conductivity (% IACS)	Tensile Strength (MPa at 24C)	Elastic Modulus (Tension GPa)
6061 T6	2.70	43%	310	68.9
2024 T6	2.77	38%	476	72.4
7075 T6	2.80	33%	572	71
3003 H14	2.73	41%	150	70

To create the detector volume (Figure 1), side rails of 3/8” by ¾” section were selected to ensure ease of fabrication. The nylon standoffs have a height of 8 ± 0.26 mm. The anode buss bar has a height of 3.175 mm (1/8”). A 19.05 ± 0.36 mm (¾”) height for the side rails ensures the anode wires will be centered in the detector volume (Figure 2). The size will also help ensure that the backplane and detector windows are sufficiently rigid to prevent deflection that could result in shorting of the anodes to the detector body.

Finally, to seal the detector body, the window frame was fabricated of 0.12” aluminum sheet. Approximately 10 cm by 10 cm square holes were created in the sheet to allow for 100 cm^2 windows. Aluminized Mylar film was adhered to the window frame to create a gas tight entrance window that would allow beta radiation to penetrate and enter the sensitive volume of the detector (Figure 3).

Detector Anode Design

The detector is a multiwire anode design in a planar configuration. The anode wires run along the 1000 mm length of the detector and are terminated in parallel to a single BNC connector at each end of the detector. Given the spacing of the anode wires, cylindrical models of proportional counters are suitable for the following calculations (Charkpak, Bouclier, Bressani, Favier, & Zupancic, 1968) (Charpak, Rahm, & Steiner, 1970).

Figure 1: Test Fitting of Detector Body Components

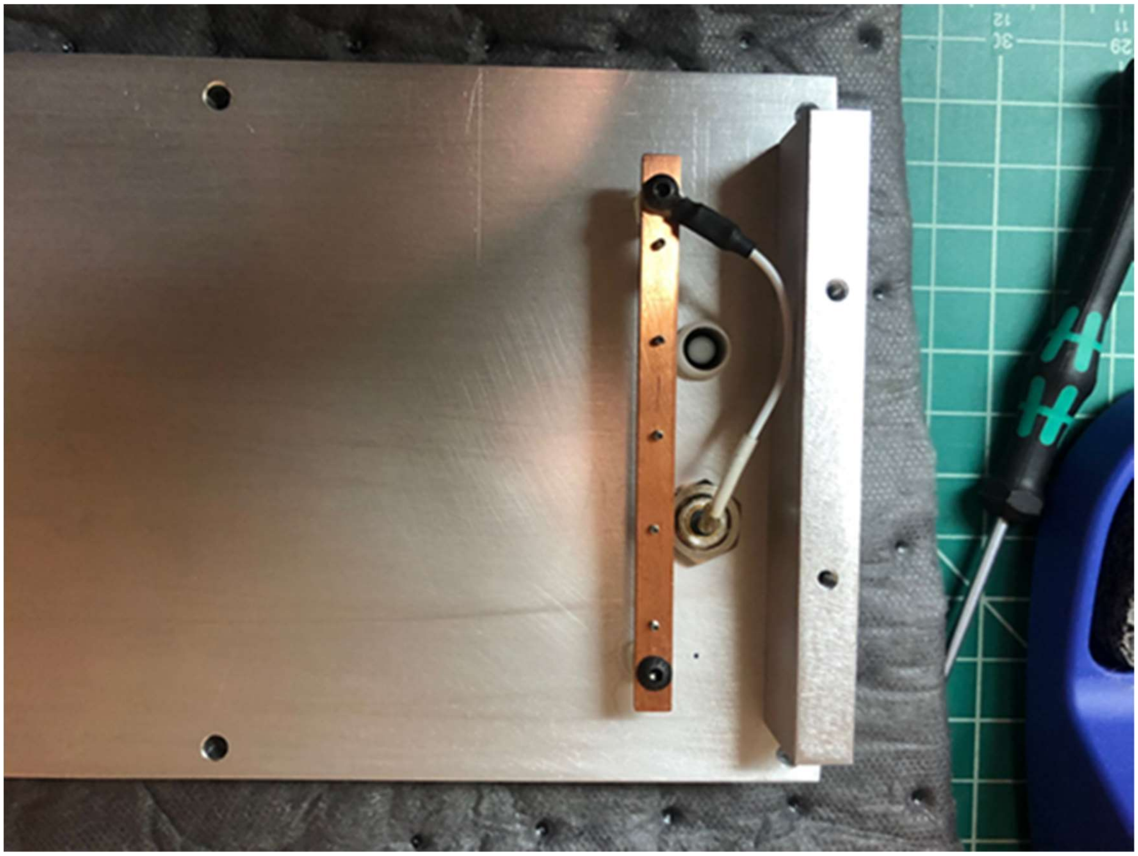

Figure 2: Anode Buss Bar and Gas Fitting Installed in Backplane of Detector

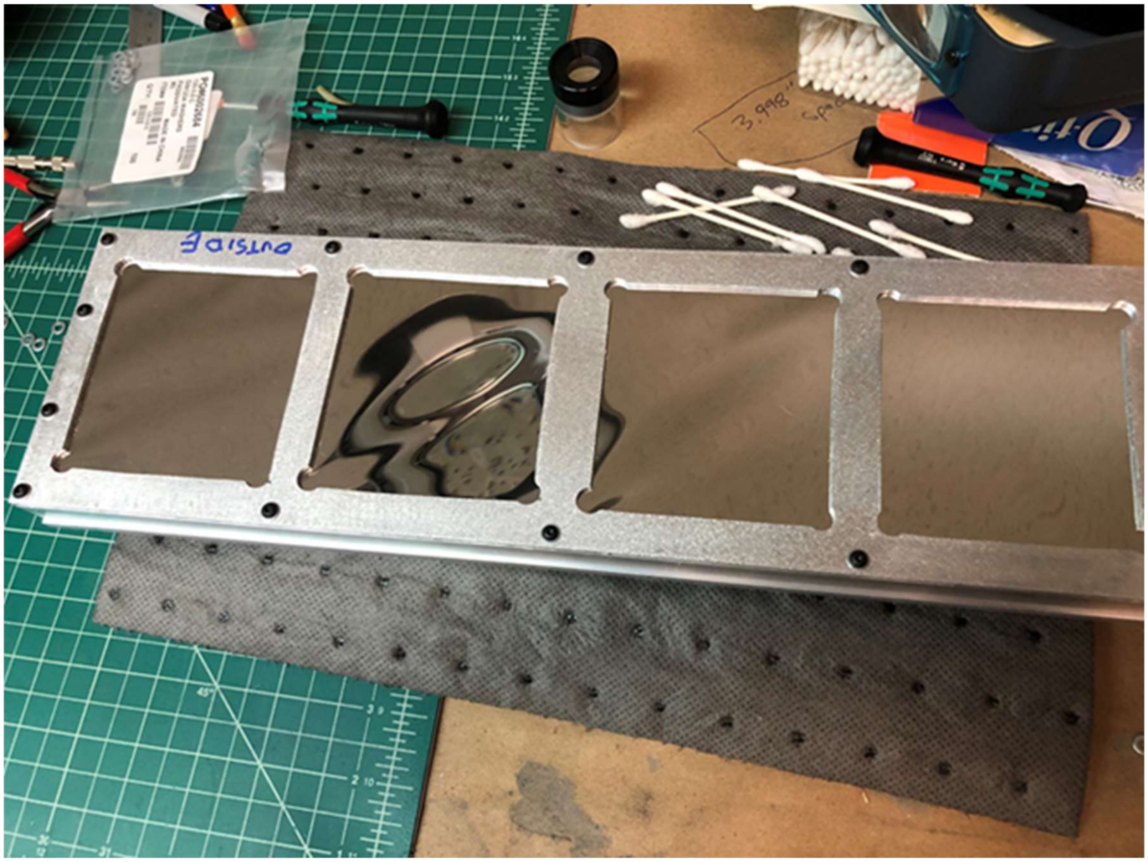

Figure 3: Detector Window Frame with Mylar Window

For position sensing applications utilizing charge division, the anode wires must be electrically resistive (Knoll, 2010). Nikrothal 80 was chosen for this application. It is 19.0 to 21.0% chromium, with small amounts of carbon, silicon, manganese, and iron, with the balance (approximately 80%) nickel. The yield strength is 400 MPa for a 1mm strip. The electrical resistivity at 20°C is 1.09 Ω mm^2 * m^{-1} (Kanthal, 2018). The nominal diameter is 0.001" (0.0254 mm). Manufacturer tolerance specifications for diameter were not provided. A sample of wire was cut from the spool and measured with a Vernier micrometer that has 0.002 mm resolution. The mean diameter is 0.023 mm (0.0009") with a sample standard deviation of 0.004 mm (0.0002") (N=10).

A circular anode wire with a nominal 0.001" (0.0254 mm) diameter has cross sectional area of 5.1 * 10^{-4} mm^2. This yields a resistance of 2151 Ω * m^{-1} for the anode wires. For a five-wire design, with the wires connected in parallel, each having a nominal length of 1 meter, the total anode resistance is approximately 430 Ω.

The second important parameter is the capacitance of the detector. Using the following equation (Leo, 1994; Sauli, 1977; Erskine, 1972) the capacitance of the anode can be calculated as

$$C = \frac{2\,\pi\,\varepsilon_0}{\frac{\pi\,G}{s} - ln\frac{\pi\,d}{s}} \tag{4}$$

where *G* is the anode to cathode distance in meters, *d* is the anode wire diameter in meters, *s* is the anode wire spacing in meters, and ε_0 is the vacuum permittivity (8.8541878128 x 10^{-12} Farads/meter (National Institute of Standards and Technology, 2019)). For this detector design, with five anode wires, each with a capacitance of approximately 7.7 pF, connected in parallel, the total capacitance is approximately 39 pF.

The tensile strength of Nikrothal 80 is 117,500 psi and the yield strength is 60,900 psi. For wires with 0.001" diameter, this gives a maximum wire tension of 0.213 N (0.048 pounds) at the yield point. The minimum necessary wire tension to ensure the anode wires do not deflect due to the electrostatic force between them is given by (Sauli, 1977) (Leo, 1994):

$$T > \frac{1}{4\pi\varepsilon_0} * \left(\frac{CVL}{s}\right)^2 \quad (5)$$

where *C* is the detector capacitance, *V* is the applied bias voltage, *L* is the length of the anode wires in meters, and *s* and ε_0 are the same as previously defined.

For this detector design, using the calculated capacitance of 39 pF and a maximum bias of 2000 volts, this results in a minimum required tension of 0.236 N. This is above the tension at the yield point of 0.213 N. Wire deflection and chamber sparking could present an issue as the bias approaches 2000 volts.

Gas System

Current gas proportional detector systems in use for decommissioning operate using P10 gas, a mixture of 10% methane and 90% argon. This detector will use P10 to maintain compatibility with current systems. Gas constants for proportional counters for P10 gas were characterized by Alkhazov et al. and Wolff. These values are W = 26 eV per ion pair (Alkhazov, Komar, & Vorob'ev, 1967) (Wolff, 1974); K = 4.8 ± 0.3 * 10^4 V * cm^{-1} * atm^{-1}; and ΔV = 23.6 ± 5.4 eV (Wolff, 1974). Using these values, the gas multiplication can be derived for the detector design as a function of applied voltage using

$$\ln(M) = \frac{V}{\ln(b/a)} * \frac{\ln(2)}{\Delta V} * \left[\ln(\frac{V}{p*a*\ln(b/a)}) - \ln(K)\right] \qquad (6)$$

where *M* is the gas amplification factor, *V* is the applied bias voltage, *a* is the anode wire radius in cm, *b* is the cathode radius in cm, *ΔV* is the potential difference in eV, *p* is the gas pressure in atm, and *K* is the minimum value of the electric field per pressure for gas amplification to occur in V * cm^{-1} * atm^{-1}. This is known as a Diethorn plot (Figure 4) (Diethorn, 1956).

The detector is designed to be operated in gas flow mode. By continually flowing P10 gas, the detector will be under a slight positive pressure, minimizing the impact of any minor leaks. Any substantial leaks will change the pressure and potentially allow contaminants into the detector, altering the gas multiplication factor.

A gas test jig was constructed to allow monitoring of the flow rate as well as the gas pressure flowing into the detector. The flow is adjustable with a needle valve. A single stage regulator with adjustable output from 0 to 15 psi was chosen for the test jig.

Given the physical design parameters and the gas selection, it is now possible to solve for the charge developed in the detector using the following equation (Knoll, 2010):

$$Q = n_o e M \qquad (7)$$

where n_0 is the number of ion pairs created, *e* is the elementary charge ($1.602176634 * 10^{-19}$ C (National Institute of Standards and Technology, 2019)), and *M* is the gas amplification factor as defined previously.

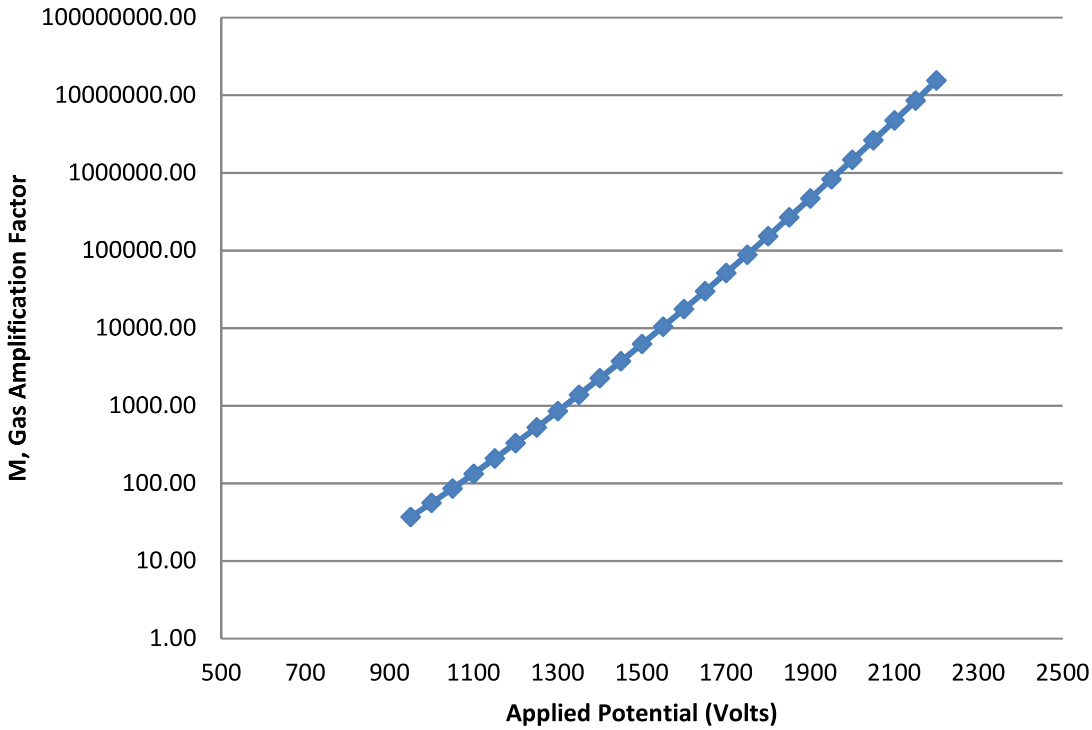

Figure 4: Diethorn Plot for P-10 Gas for This Detector Design

For P10 gas, W=26 eV (Wolff, 1974; Alkhazov, Komar, & Vorob'ev, 1967), using the average beta energy of C-14 (49.16 keV), approximately 1891 ion pairs will be created prior to any gas multiplication, assuming all of the beta energy produces ions in the sensitive volume of the detector. Using the maximum beta energy of Y-90, approximately 87,642 ion pairs will be created. At 1000 volts, the gas multiplication, M, will be approximately 56. At 2000 volts, M will be approximately $1.47 * 10^{6}$. As a result, the total charge created, Q, will range from $1.7 * 10^{-14}$ to $2.1 * 10^{-8}$ C. Practically, however, to minimize space charge effects, the detector should be operated at lower levels of gas amplification (Hendricks, 1969).

Chapter 4

Results and Discussion

Detector Resistance

The calculated resistance for the anode wires, from BNC terminal to BNC terminal was 430 Ω. The measured resistance using a Fluke 117 digital multimeter is 415 Ω (Fluke Corporation, 2006). The two critical parameters in calculating the resistance were anode wire diameter and length. The measured resistance suggests that the values used for anode wire diameter and length are reasonably accurate.

Detector Capacitance

The calculated capacitance for the detector is approximately 39 pF. The measured capacitance using a BK Precision Capacitance meter is 54.1 (±1.5) pF (BK Precision Corp, 2011). This value is substantially larger than the calculated result and warrants further investigation.

The three critical values in calculating the capacitance are anode wire diameter, anode wire spacing, and anode to cathode distance. The resistance measurement suggests that the anode wire diameter is accurate. A sensitivity analysis was performed on anode wire spacing and anode to cathode distance. A 10% increase in spacing results in an increase in capacitance of 1%. A 10% increase in anode to cathode distance results in a decrease in capacitance of 3%. It seems unlikely that error in spacing or anode to cathode distance has resulted in the error in capacitance.

Using the measured value of detector capacitance, the minimum required tension found using Equation 5 is 0.484 N for an applied bias of 2000 volts. This is far in excess of the maximum tension at the yield point for the anode wire of 0.213 N. By setting $T_{min} < T_{yield}$ and solving for voltage, the maximum bias that can be applied is 1300 volts, assuming the anode wires were able to be installed at their maximum tension.

Preamplifier Characterization

Charge sensitive preamplifiers were selected to ensure compatibility with the charge division method of position sensing. Cremat, Inc offers charge sensitive preamplifier modules. The modules were selected because they have the potential to be useful for field portable instruments. There are several modules with different levels of gain available. The CR-110-R2 modules were selected because it offers the largest gain (Cremat, Inc, 2014).

The two Cremat, Inc preamplifiers were tested for proper operation and consistency by connecting them to a Siglent SDG1032X Arbitrary Waveform Generator in accordance with the application sheet (Cremat, Inc, 2014). The waveform generator was set to square wave output at 1 kHz, 500 mV peak to peak with a 50% duty cycle. This pulse was fed into each preamplifier one at a time to the test input. The output from the preamplifiers were connected to the oscilloscope with a 50 Ω terminator. The results are presented in the table below (Table 3):

Table 3: Preamplifier Rise Times

	Rise Time (ns)	Standard Deviation (ns)
Preamplifier A	3.95	0.22981
Preamplifier B	3.92	0.28818

The additional capacitance of a detector and coaxial cable at the input of the preamplifier will cause a longer rise time. The specification sheet value is 0.4 ns * pF^{-1} (Cremat, Inc, 2014). For a detector with 39 pF, we can expect the rise time will be slowed by an additional 15.6 ns. For a detector with a 54.1 pF capacitance, the rise time will be slowed by an additional 21.64 ns. A 36" long RG-58C/U coaxial cable will have a nominal capacitance of 100.1 pF * m^{-1} (Knoll, 2010). Using a BK Precision Capacitance meter, the measured value for the coaxial cable was 94.1 (±1.9) pF. By measuring the rise times of the pulses for each preamplifier with nothing connected to the input, then again with a 36" coaxial cable connected to the input, and finally with a 36" coaxial cable and detector connected to the input, it will be possible to verify both the specification sheet value of 0.4 ns * pF^{-1} as well as the actual detector capacitance value (39 versus 54.1 pF).

For the 36" coaxial cable connected to the preamplifier inputs, the rise times are presented in the table below (Table 4) along with the difference in rise time from the initial rise time test with nothing connected to the preamplifier input and the change in rise time divided by the measured coaxial cable capacitance.

The calculated change in rise time per unit of capacitance (approximately 0.2 ns * pF^{-1}) agrees with the specification sheet value of 0.4 ns * pF^{-1} given the effect of the 50 Ω termination into the oscilloscope. Next, a 36" coaxial cable was used to connect the detector to the input of the preamplifier and rise times were once again measured. The table below (Table 5) presents the rise times, the change in rise time from the previous

Table 4: Preamplifier Rise Times with 36" Coaxial Cable Connected to Input

	Rise Time (ns)	**Standard Deviation (ns)**	**Change in Rise Time (ns)**	**Calculated Change (ns/pF)**
Preamplifier A	22.53	0.50592	18.58	0.19745
Preamplifier B	22.52	0.54325	18.60	0.19766

experiment and the change in rise time per unit of capacitance using the measured detector capacitance of 54.1 pF.

The calculated change in rise time per unit of capacitance using the detector capacitance value of 54.1 pF is again approximately 0.2 ns * pF^{-1} before considering the 50 Ω terminator. This provides confirmation of both the specification sheet value for change in rise time with added capacitance as well as the true value of detector capacitance being 54.1 pF and not the calculated value of 39 pF.

Next, each preamplifier was tested for equivalent noise charge (ENC) using the procedure in the specification sheet (Cremat, Inc, 2014). The specified ENC is 270 electrons RMS or 0.04 fC RMS. The preamplifier output was connected to an Ortec 570 Linear Amplifier with a 1 µs shaping time and a gain of 10. The output of the amplifier was connected to the oscilloscope via a 50 Ω terminator, AC coupled, and the RMS voltage was measured. The preamplifier specifications are a gain of 1.4 volts * pC^{-1} (Cremat, Inc, 2014). The characteristics of the two preamplifiers are presented in the following table (Table 6). These noise values are in good agreement with the specification sheet values.

Testing System Noise

Ortec 460 Amplifiers were selected for the position sensing system. The two amplifiers were tested for noise per the manual and were within specification (ORTEC, 2002). The first test was to determine the noise of the system at the three available integrating times of the Ortec 460 amplifier.

Table 5: Preamplifier Rise Times with 36" Coaxial Cable and Detector Connected

	Rise Time (ns)	**Standard Deviation (ns)**	**Change in Rise Time (ns)**	**Calculated Change (ns/pF)**
Preamplifier A	33.83	1.58	11.30	0.20887
Preamplifier B	34.69	1.48	12.17	0.22495

Table 6: Preamplifier Equivalent Noise Charge

	Number of Measurements	**RMS Voltage (µV)**	**Standard Deviation (µV)**	**ENC (fC)**	**ENC (electrons)**
Preamplifier A	1012	679.67	307.23	0.049	303
Preamplifier B	1007	644.65	292.82	0.046	287

One preamplifier was connected to the detector and an Ortec 460 amplifier. The amplifier was connected to the oscilloscope via a 50 ohm terminator, AC coupled, to measure noise at various levels of gain and with the three integrating times. Results are presented in the following graph (Figure 5). System noise is clearly minimized by using the 0.25 μs integrating time on the amplifier.

The next noise test was for the detector in position sensing configuration. The detector was connected to both preamplifiers with a 6 inch coaxial cable. Each preamplifier was connected to an amplifier set at 0.25 μs integrating time. The amplifier unipolar outputs were connected to the oscilloscope via 50 ohm terminators, AC coupled, for noise measurements. The results are presented in the table below (Table 7).

An important point to note is that the noise performance in this configuration is approximately ten times greater than the noise of the system in a single ended configuration. The severe noise will be problematic for position determination.

Determining Detector Operating Voltage

The detector was connected to a single preamplifier. The preamplifier output was connected to an Ortec 570 amplifier set to 1 μs shaping time and a gain of 1500. The output of the amplifier was fed to an Ortec 550 single channel analyzer (SCA). The SCA was set up to be a discriminator and transform the Gaussian shaped pulse from the amplifier into a square shaped pulse for a frequency counter to analyze.

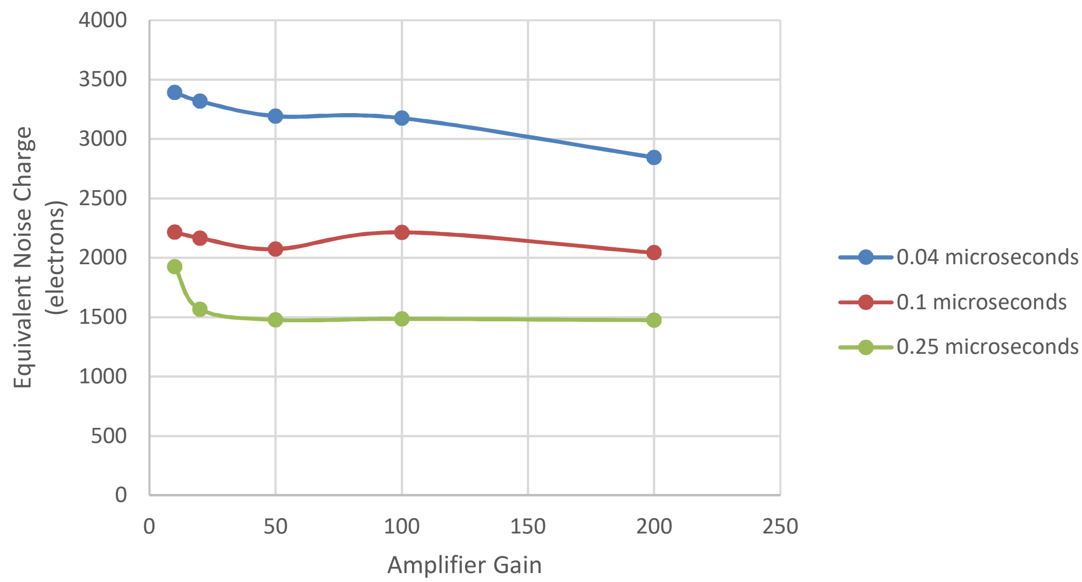

Figure 5: System Noise Testing

Table 7: Position Noise Measurements

Amp Gain	Preamp	N	Mean (V)	SD (V)	ENC (fC)	ENC (electrons)
1000	A	1045	3.63	1.01	2.592857	16183.34
1000	B	1079	3.25	1.09	2.321429	14489.22
10	A	1049	0.03549	0.00785	2.535	15822.23
10	B	1028	0.04087	0.00929	2.919286	18220.75

An Ortec high voltage power supply was connected to one of the preamplifiers. All coaxial cables were RG-58C/U.

An Fe-55 source with a nominal activity of 1 μCi (37,000 Bq) ± 20% (Spectrum Techniques, LLC, 2019) was selected for this test. Fe-55 emits a 5.89875 keV x-ray during 16.57% of the disintegrations and a 5.88765 keV x-ray during 8.45% of the disintegrations (Be M.-M. a., 2006). This is approximately a monoenergetic source.

An Sr-90 source with a nominal activity of 0.1 μCi (3,700) ± 20% (Spectrum Techniques, LLC, 2019) was selected for this test. Sr-90 decays into Y-90. Due to the short half life of Y-90, it will be found in secular equilibrium with the Sr-90. Sr-90 and Y-90 are both beta emitting isotopes. Y-90 has a maximum beta energy of 2,278.7 keV and Sr-90 has a maximum beta energy of 545.9 keV (Be M.-M. a., 2006).

The bias voltage was applied in 50 volt increments from 900 to 1150 volts. Additionally, bias voltages were selected to ensure that the calculated maximum bias of 1300 volts is not approached in order to avoid detector and/or preamplifier damage. The background count rate was measured with the frequency counter. The Fe55 source was placed in under the center of the detector and the count rate was measured. The Fe55 source was replaced with a Sr90 source and the count rate was measured. The minimum detectable count rate (MDCR) was calculated using

$$MDCR = 3 + 4.65\sqrt{B} \tag{8}$$

where B is the background count rate (Strom & Stansbury, 1992) (Currie, 1968). The results are plotted in Figure 6. Fe-55 is difficult to detect and requires more gas

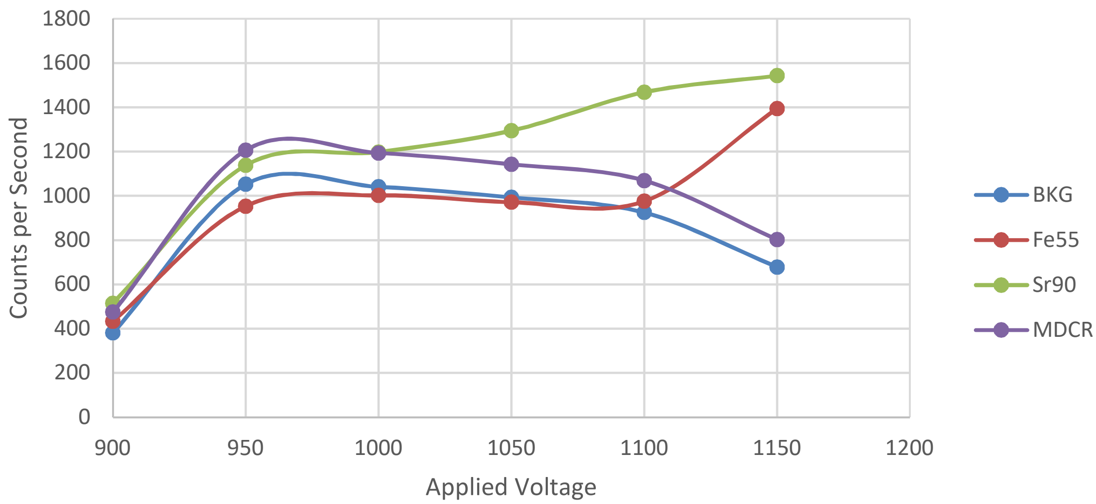

Figure 6: Background, Iron-55, Strontium-90, and Minimum Detectable Count Rates

amplification than the Sr-90. The count rate for Sr-90 began to exceed the MDCR at 1000 volts while the Fe-55 did not exceed the MDCR until 1150 volts.

Testing Calculated Values of the Gas Amplification Factor

Using Equation 7, and the P-10 gas W value of 26 eV per ion pair created, the total charge created in the detector can be calculated for an Fe-55 x-ray. Ignoring gas amplification, the charge produced will be $3.63 * 10^{-5}$ pC. The Cremat preamplifier has a gain of 1.4 volts * pC^{-1} (Cremat, Inc, 2014), and the Ortec 570 maximum gain is 1500 (ORTEC, 2002). The expected signal output for an Fe-55 x-ray that loses 100% of its energy in the sensitive volume of the detector is 76.23 mV before any gas amplification. By using the Diethorn plot in Figure 4, the gas amplification for a bias of 1150 volts was determined to be approximately 209. The expected signal output would be 16 volts. The amplifier is only able to produce signals up to 10 volts. This suggests that the gas amplification is less than anticipated.

The SCA was set to a 0.5 volt window and swept from 0 volts to 10 volts to count background and the Fe-55 source. The results are displayed in the graph below (Figure 7). The Fe-55 source count rate exceeded the MDCR from 0 to 1.5 volts. If we assume that the Fe-55 x-ray produced an output pulse at 1.5 volts, and divide by the expected signal output of 76.23 mV prior to gas amplification, this yields an approximate gas amplification of 20, or a factor of 10 less than initially predicted.

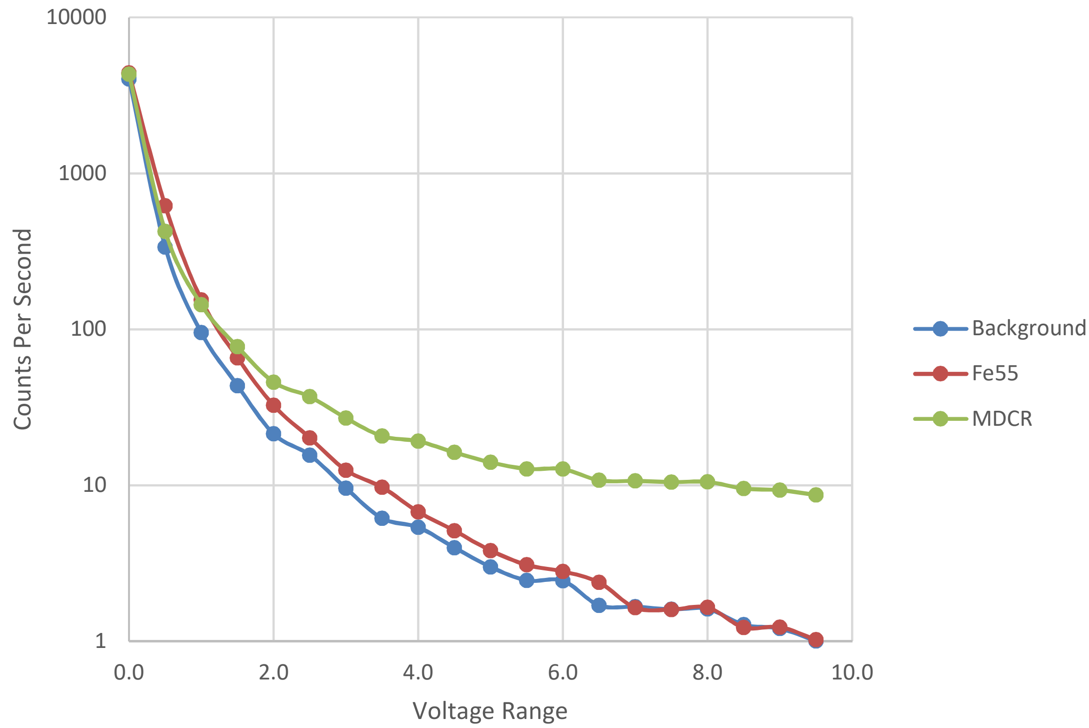

Figure 7: Single Channel Analyzer Output from 0 to 10 Volts with a 0.5 Volt Window

Further Investigation of Noise in the Position Sensing Configuration

A key design parameter was missed during the design and build of the first phase prototype. Anode wires should not be connected in parallel for charge division position sensing. When using resistance-capacitance position encoding, resistors can be used to connect the anodes in parallel and a system of four preamplifiers can be used, with some distortion (Borkowski & Kopp, 1975).

After realizing the error, four anodes were removed from the detector, leaving the central anode in place. During this procedure, the Mylar entrance window was inspected for any signs of spark damage. Signs of the aluminum being eroded from the Mylar were found and can be seen in the photo below (Figure 8).

After repairing the Mylar entrance window, the detector was reassembled and tested for function with a single preamplifier. First, the high voltage plateau was established at two different lower level discriminator levels; 200 mV and 300 mV. Then Fe55 and Sr90 source counts were collected. The results are presented in the graph below (Figure 9).

The next test was for noise performance in the position sensing configuration as presented before. The detector was connected to both preamplifiers, the high voltage was applied, and an oscilloscope trace was captured. During the capture one of the preamplifiers was destroyed. At this point, testing no further testing was performed. The trace is presented in the graph below (Figure 10).

Figure 8: Spark Damage to Mylar Window

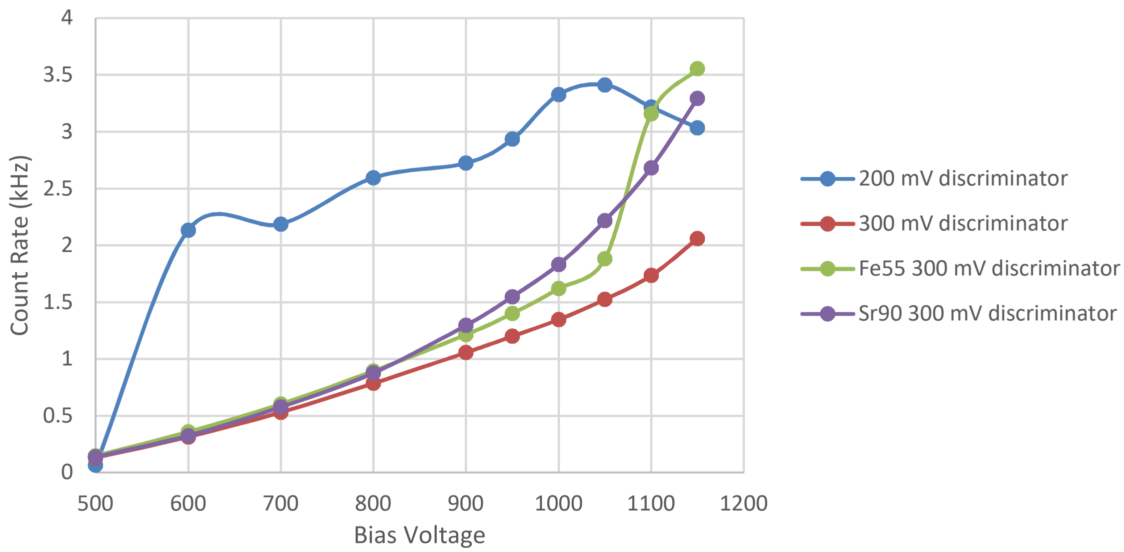

Figure 9: Background and Source Count Rates

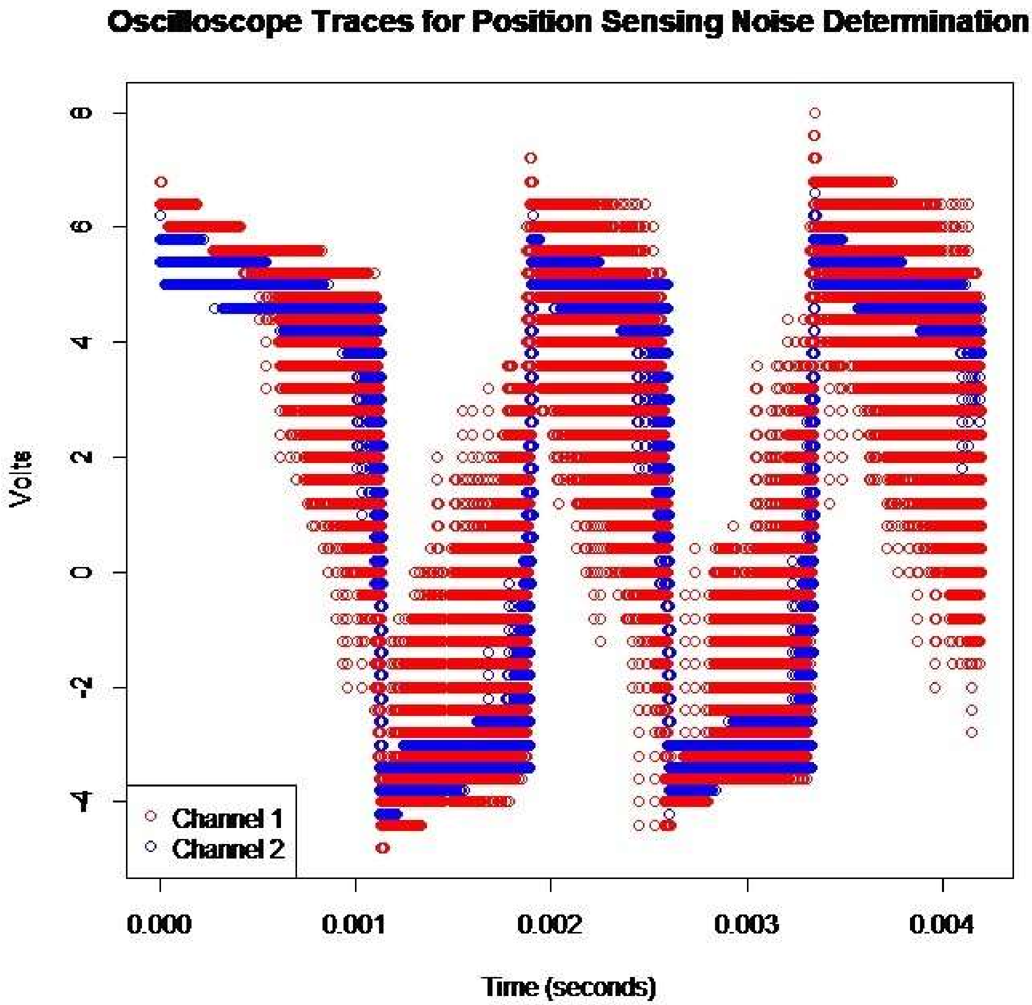

Figure 10: Oscilloscope Trace During Position Noise Testing

Chapter 5

Conclusions

The design and build of a position sensing gas proportional detector is the first step in achieving an instrumentation system that will reduce labor costs and increase accuracy of final status surveys during decommissioning of surface contaminated facilities. This work set out to review the literature on the topic, design and build a first prototype and develop an understanding of key design criteria for the construction of a position-sensitive gas proportional detector appropriate for decommissioning.

The difference between the calculated and measured capacitance of the detector as well as the difference between the calculated and measured gas amplification revealed some design and build issues. Critical parameters that must be tightly controlled in a successful design include the anode wire diameter, the anode wire length, the anode to cathode distance, and the anode wire spacing. The anode to cathode distance should be greater than the anode wire spacing, by a factor of three to four (Sauli, 1977).

To ensure those parameters are tightly controlled, the tolerances on the cathode back plane flatness, the perpendicularity of mounting holes, the height of insulating standoffs, the height of the anode buss bar, the position and diameter of the anode wire mounting holes in the anode buss bar, and the height, flatness, and parallelism of the cathode side rails need to be examined and optimized to minimize the impacts of tolerance stacking and cost to manufacture while maximizing ease of assembly and repair.

The ENC measurements revealed that position sensing is not possible with the current system. Noise performance is a critical parameter that must be further investigated, and only then can a preamplifier be specified.

Recommended Future Work

The five-anode wire design of the first prototype requires ten preamplifiers to function. A cost analysis will be necessary to determine if a multiwire design can offer enough benefits, such as a reduction in background count rate, an increase in scanning speeds, or higher quality position sensing than a single wire design. It will likely be worthwhile to develop both a single wire prototype detector as well as a multi-wire prototype detector to compare these factors.

Control of capacitance is important to ensure that a wide detector can operate at a sufficiently high voltage to ensure a gas amplification on the order of 10^2. This may also have additional effects on the preamplifier design due to the decreased amount of electronic gain necessary for good signal.

A study of resistive materials such as stainless steels and other nickel chromium alloys is necessary. Yield strength is a key parameter to ensure sufficient tension to prevent deflection and sparking. Resistance per unit length is another critical performance parameter, especially because resistance has noise implications.

Finally, this work considered the detector and preamplifiers as separate concepts. The results clearly indicate that preamplifier design or selection require a significant amount of work. The noise of the detector is such an important design value for preamplifiers that they should not be considered separately from the detector design.

List of References

Alberi, J., & Radeka, V. (1976). Position Sensing by Charge Division. *IEEE Transactions on Nuclear Science*, 251-258.

Alkhazov, G., Komar, A., & Vorob'ev, A. (1967). Ionization Fluctuations and Resolution of Ionization Chambers and Semiconductor Detectors. *Nuclear Instruments and Methods*, 1-12.

American Society of Mechanical Engineers. (2013). *B1.20.1 Pipe Threads, General Purpose, Inch.* American National Standards Institute.

ASM International. (1990). *ASM Handbook, Volume 2: Properties and Selection: Nonferrous Alloys and Special-Purpose Materials.* ASM International.

Be, M.-M. a. (2006). *Table of Radionuclides Volume 3, Monographie BIPM-5.* Sevres, France: Bureau International des Poids et Mesures.

Be, M.-M. a. (2013). *Table of Radionuclides Volume 7, Monographie BIPM-5.* Sevres, France: Bureau International des Poids et Mesures.

Be, M.-M., Chiste, V., Dulieu, C., Browne, E., Chechev, V., Kuzmenko, N., . . . Dersch, R. (2004). *Table of Radionuclides Volume 1: A = 1 to 150.* Sevres, France: Bureau International des Poids et Mesures.

BK Precision Corp. (2011). *Data Sheet: 11,000-Count Dual-Display Handheld Capacitance Meters 830C and 890C.* BK Precision Corp.

Borkowski, C., & Kopp, M. (1968). New Type of Position-Sensitive Detectors of Ionizing Radiation Using Risetime Measurement. *Review of Scientific Instruments*, 1515-1522.

Borkowski, C., & Kopp, M. K. (1975). Design and Properties of Position-Sensitive Proportional Counters Using Resistance-Capacitance Position Encoding. *Review of Scientific Instruments*, 951-962.

Charkpak, G., Bouclier, R., Bressani, T., Favier, J., & Zupancic, C. (1968). The Use of Multiwire Proportional Counters to Select and Localize Charged Particles. *Nuclear Instruments and Methods*, 262-268.

Charpak, G., Rahm, D., & Steiner, H. (1970). Some Developments in the Operation of Multiwire Proportional Chambers. *Nuclear Instruments and Methods*, 13-34.

Cremat, Inc. (2014, May). CR-Z-110 and CR-Z-110-HV CSP Instruments: Application Guide. West Newton, MA.

Currie, L. A. (1968). Limits for Qualitative Detection and Quantitative Determination: Application to Radiochemistry. *Analytical Chemistry*, 586-593.

Diethorn, W. (1956). *A Methane Proportional Counter System for Natural Radiocarbon Measurements.* Pittsburgh, PA: Carnegie Institute of Technology.

Erskine, G. (1972). Electrostatic Problems in Multiwire Proportional Chambers. *Nuclear Instruments and Methods*, 565-572.

Fano, U. (1947). Ionization Yield of Radiations. II. The Fluctuations of the Number of Ions. *Physical Review*, 26-29.

Fluke Corporation. (2006). *Fluke 11X Series Digital Multimeters Extended Specifications.* Fluke Corporation.

Foeth, H., Hammarstrom, R., & Rubbia, C. (1973). On the Localization of the Position of the Particle Along the Wire of a Multiwire Proportional Counter. *Nuclear Instruments and Methods*, 521-524.

Hendricks, R. W. (1969). Space Charge Effects in Proportional Counters. *The Review of Scientific Instruments*, 1216-1223.

Kanthal. (2018, July 6). Nikrothal 80 Strip Datasheet. Sandvik Group.

Knoll, G. F. (2010). *Radiation Detection and Measurement.* Danvers, MA: John Wiley & Sons, Inc.

Leo, W. (1994). *Techniques for Nuclear and Particle Physics Experiments: A How To Approach.* New York: Springer-Verlag Berlin Heidelberg GmbH.

Mori, C., Uno, M., & Watanabe, T. (1982). Self-Induced Space Charge Effect on Gas Gain in Proportional Counters. *Nuclear Instruments and Methods*, 49-52.

National Institute of Standards and Technology. (2019, May 31). *The NIST Reference on Constants, Units, and Uncertainty*. Retrieved from https://www.nist.gov/pml/fundamental-physical-constants

ORTEC. (2002). *Model 460 Delay Line Amplifier Operating and Service Manual.* Advanced Measurement Technology, Inc.

ORTEC. (2002). *Model 570 Spectroscopy Amplifier Operating and Service Manual.* Advanced Measurement Technology, Inc.

Pasternack Enterprises, Inc. (2017). RF Connectors Technical Data Sheet PE4077 REV 1.4. Irvine, CA.

Ramo, S. (1939). Currents Induced by Electron Motion. *Proceedings of the I.R.E.*, 584-585.

Rice-Evans, P. (1974). *Spark, Streamer, Proportional and Drift Chambers.* London: The Richelieu Press.

Rossi, B. B., & Staub, H. H. (1949). *Ionization Chambers and Counters Experimental Techniques.* New York: McGraw-Hill Book Company, Inc.

Sauli, F. (1977). *Principles of Operation of Multiwire Proportional and Drift Chambers.* Geneva: CERN.

Schubelin, P., Fuhrmann, J., Iwata, S., Radeka, V., Schreiner, W., Turkot, F., & Weitsch, A. (1975). Low Mass Cylindrical Multiwire Proportional Chamber with Unambiguous Dual Coordinate Readout. *Nuclear Instruments and Methods*, 39-46.

Shockley, W. (1938). Currents to Conductors Induced by a Moving Point Charge. *Journal of Applied Physics*, 635-636.

Spectrum Techniques, LLC. (2019). *Alpha/Beta/X-ray Laminate Disk Sources*. Retrieved from Spectrum Techniques, LLC : http://www.spectrumtechniques.com/products/sources/laminate-sources-ldslcc-series/

Strom, D. J., & Stansbury, P. S. (1992). Minimum Dtectable Activity When Background is Counted Longer than the Sample. *Health Physics*, 360-361.

United States Department of Defense, Department of Energy, Environmental Protection Agency, and Nuclear Regulatory Commission. (2000). *Multi-Agency Radiation Survey and Site Investigation Manual.* Washington DC: US Government Printing Office.

Wolff, R. S. (1974). Measurement of the Gas Constants for Various Proportional-Counter Gas Mixtures. *Nuclear Instruments and Methods*, 461-463.

Vita

Christopher Echterling attended Indiana University in Bloomington and graduated with a Bachelor of Science degree in 2004. He worked in radiation safety for Indiana University from 2003 until 2008. He attended the Kelley School of Business at Indiana University and graduated in 2009 with a Master of Business Administration and a graduate certificate in International Business Management. During his time at Kelley, he studied at WHU – Otto Beisheim School of Management in Vallendar, Germany and the Pontifical Catholic University of Chile in Santiago, Chile. Upon returning to the United States, Christopher worked as a Health Physicist at Purdue University in West Lafayette, Indiana from 2010 until the end of 2011. While working for Purdue he enrolled in the Master of Science program in Health Physics at Purdue. In 2011, Christopher accepted a position as the Corporate Radiation Safety Officer for Chase Environmental Group, located in Oak Ridge, TN. Christopher transferred to the Master of Science program in Radiological Engineering at the University of Tennessee Knoxville via the distance education program and graduated in the spring of 2020.